Evaluation of Density Functional Theory in the Bond Rupture of Octane

E. GOLDSTEIN,[1] M. HAUGHT,[2] Y. TANG[2]

[1]*Department of Chemistry, California Polytechnic University at Pomona, 3801 West Temple, Pomona, California 91768*
[2]*Chevron Petroleum Technology Co., La Habra, California*

Received 4 June 1997; accepted 14 July 1997

ABSTRACT: Density functional methods at the 6-31G* level are applied to the rupture of *n*-octane into methyl–heptyl, ethyl–hexyl, propyl–pentyl, and butyl–butyl radical fragments. The energetics of the radicals at UMP3, UMP2/6-31G*//UHF/6-31G* (hereafter referred to as UMP), are compared to UB3LYP/6-31G* results (referred to as UB). Although the UMP approach matches additivity energies to within 5 kcal/mol, it fails to mimic the overall energetic trend. The UB energies agree with additivity estimates and trends to within 1–2 kcal/mol and radical entropies deviate by only 2 e.u. from available experimental data. © 1998 John Wiley & Sons, Inc. *J Comput Chem* **19**: 154–167, 1998

Keywords: density functional theory; free radicals; alkane fragmentation

Introduction

Alkyl radicals play an important role in the petroleum industry[1] and are reactive intermediates in the production of many commercial polymers. Previous studies of radicals include gas phase kinetics of bond fission processes,[2] spectroscopic analysis, chemical reactivity, and theoretical calculations.[3, 4] In refineries, it is particularly important to model thermal cracking of catalytic processes. Oil and gas explorations use hydrocarbon cracking models to predict the thermal deadline of oil with burial depth. Because the process of oil cracking occurs under low geothermal temperature (roughly 150°C) over long periods of time, it is impossible to simulate it directly under laboratory conditions. Therefore, an accurate kinetic model is essential for extrapolation of laboratory conditions unto a geological framework. However, due to the complexity of the cracking process, it is impossible to derive a unique kinetic solution without constraining some kinetic parameters. Thus, *ab initio* calculations play an important role in constraining relative energy barriers for the different bond-breaking processes. Previously, third law calculations[5a] were used to compute entropies of C3 or

Correspondence to: E. Goldstein; e-mail: egoldstein@csupomona.edu

CCC 0192-8651 / 98 / 020154-14

C4 fragments, which in turn require knowledge about symmetry, barriers for internal rotation, and other parameters leading to low-energy vibrational frequencies.[3a] These were then used to obtain the free energy of the cracking process, but provided only limited information.

In this study, a detailed study of carbon–carbon homolytic bond cracking of *n*-octane (C8) will be discussed. This study does not attempt to match the direct extrapolation of oil cracking under laboratory or geological conditions, but rather provide some theoretical constraints for kinetic parameters derived from laboratory simulation. The present investigation focuses on the clarification of the energetic trends of the rupture of octane to primary radicals. Due to a lack of sufficient thermochemical data and disagreements between theory and additivity predictions, questions exist on the C8 bond ruptures. We hope to resolve some of these discrepancies with the use of DFT methods.

A minor application relates to locating a preferable carbon–carbon bond rupture point in larger primary hydrocarbons. This is of practical use in systems exceeding a C30 chain, and involves identifying a point amenable to rupture. Thus, instead of focusing on energetics, a relative trend of bond dissociations would be useful as a simpler and less time-consuming method for the study of preferential C—C bond ruptures in these larger systems.[6] This is tested for validity by comparing the octane fully optimized DFT approach to the snapshot effect, or approach II, which simply elongates the ruptured bond. The relative energetics trends of the snapshot approach are not expected to be accurate, but if bond strength trends remain consistent with the DFT approach, a simpler, more practical method may be available for C30 and higher hydrocarbons.

Low-temperature cracking experiments of alkane radicals lack information on the bond rupture positions. As experimental studies of the structures of alkane radicals have been greatly facilitated by isolating them at cryogenic temperatures in halocarbon matrices, and this has also resulted in Jahn–Teller distortions.[3c,7] The question of whether these distortions are due to isolated radical or matrix effects has not yet been resolved. All of these difficulties make the problem especially suitable to theoretical predictions, which are able to determine the structures of isolated radicals.

It has been notoriously difficult to reproduce the bond rupture differences computationally as both dynamic and nondynamic correlation energy need to be included to obtain reasonable energies.[8] This is a general problem in the study of bond rupture reactions, which include closed-shell (octane) and open-shell (radical) species. Recently, density functional theory (DFT) with gradient nonlocal corrections has been shown to be a relatively economical way to calculate bond dissociation energies.[9] Successful calculations of singlet–triplet gaps in carbenes and related species are an indication that DFT can handle energy differences between closed-shell and open-shell species.[10–13] These features of DFT suggest that it might also prove useful in balancing the energies of *n*-octane and the series of doublet radicals. As will be shown here, the Becke3LYP functional with the 6-31G* basis set produces excellent geometries and energies for both C8 and resulting radicals. This opens up the whole field of bond ruptures beyond primary alkanes, which will yield valuable industrial and synthetic predictions beyond the closed-shell DFT regime.[9]

Until recently, theoretical studies of the alkane bond dissociation reaction to radicals have ranged from force-field studies[4b,c] to *ab initio* techniques that include Hartree–Fock (HF), and post-HF methods.[4] The *ab initio* studies show qualitative agreement on geometries and energies of the radicals' heats of formation, whereas RHF calculations with limited CI give somewhat similar results for the radical energies.[1] For radicals, UHF, as well as dynamic correlation corrections, are necessary to provide even qualitatively reasonable results.[4c] Restricted Hartree–Fock (RHF) favors the closed shell whereas unrestricted Hartree–Fock (UHF) and semiempirical treatments are biased toward radicals, thus it is necessary to apply a method that yields a balanced treatment of closed-shell and radical (open-shell) mechanisms.[3,8] Although post-HF computations have succeeded in providing accurate results, the requirements in terms of computation time are highly demanding. For the *n*-octane successive bond ruptures, it is especially costly to include all configurations for all resulting species.

Methyl groups bonded to a radical center exert a profound influence on both structure and stability of the trigonal site. The nature and magnitude of the interactions involved will be studied here in detail with energies, vibrational frequencies, and geometries of the methyl through heptyl radical centers.[14a] Previous studies utilizing ESR found the spin density to decrease for CH3 > CH3CH2 > CH2H5CH2.[14b] This trend reveals the constraints on the unpaired electron to be orthogonal

to the C—H orbitals of the same symmetry. The question remains to what extend CH_3 substituents induce nonplanarity in a series of primary radicals. Conformational disorder in the form of low-concentration *gauche* C—H bonds was found to occur primarily near the ends of the chain.[14c] These questions have been detailed previously, and here we investigate the utility of DFT in elucidating radical geometries and frequencies.

The thermodynamic and kinetic stability of these primary radicals is centered about their heats of formation. It was previously demonstrated that experimental kinetic data for decomposition of primary alkanes is incompatible with the ΔH_f^0 values. Specifically, ΔH_f^0 values were 10–20 kJ/mol higher than required.[5a] Benson's additivity method,[5b,c] with recent modifications by Leroy and Sana,[5d] is widely accepted as a simple approach for estimating thermodynamic properties of molecules, especially heats of formation. We shall refer to this method as the ''modified additivity scheme.'' When group contribution values have been estimated with sufficient experimental data, estimates of heats of formation are typically within 2 kcal/mol of the observed values. However, if an acceptable database is not available, group values are either missing or poorly known, rendering the modified additivity method inaccurate. This is the case for the primary alkyl radicals family of compounds. Clearly, this method could be enriched with G2-level calculations and ideal gas phase heats of formation calculated at any temperature.[15] This option was not found to be a desired approach here as it consists of a number of correction terms added to a base calculation of MP4/6-311G** and QCISD(T) corrections. To extend an efficient and more practical approach to primary alkyl radicals resulting from rupture of linear or, in the future, cyclic alkanes, we turned to MP2 or MP3 UHF techniques and DFT methods.

The empirical gas phase ΔH_f^0 (standard enthalpy of formation at 1 atm, 298.15 K) of propyl, butyl, pentyl, hexyl, and heptyl radicals were estimated according to the following scheme:[16–18] If the C8 rupture to $\cdot$C2 + $\cdot$ C6 is used as an example,the heat of formation of the hexyl radical (unknown experimentally) must be determined using the additivity scheme: D (H—C6H13) = ΔH_f^0[$\cdot$C6H13] + ΔH_f^0[$\cdot$H] − ΔH_f^0[C6H14] and D (H5C2—C6H13) = ΔH_f^0[$\cdot$C2H5] + ΔH_f^0[$\cdot$C6H13] − ΔH_f^0[C8H18].

With the heats of formation of the hydrogen radical equal to 52.1 kcal/mol, hexane −39.92 kcal/mol, octane −49.9 kcal/mol, ethyl radical 27.80 kcal/mol, and an averaged dissociation energy for H—C6H13 of 100.2 kcal/mol, the heat of formation of the hexyl radical is estimated to be 8.18 kcal/mol. This results in a C—C rupture of 85.8 kcal/mol. The minimum deviation using these modified additivity rules is less than 2 kcal/mol. This may be due to the exclusion of conformational mixing under standard conditions, with only the energetically most stable conformer considered. It is of interest to note that the C2—C6 rupture yields a value of 86.23 kcal/mol using MM3.[4b,c] This deviates from the modified additivity scheme by less than 0.4 kcal/mol.

Computational Methods

Calculations were performed with the Gaussian-94/DFT series of programs.[19] The DFT hybrid functional, Becke3LYP, consists of the nonlocal exchange functional of Becke's three-parameter set[20] and nonlocal correlation functional of Lee, Yang, and Parr.[21] All functionalities are employed with self-consistent field HF densities. The 6-31G* basis was used in all calculations.[19]

Full geometry optimizations were performed with conventional Gaussian default convergence criteria for all structures. The total electronic energy of each radical was computed at the optimized geometry. Bond lengths and bond angles of interest are tabulated in Tables I and II. The tabulation of bond lengths and bond angles for butyl, pentyl, hexyl, and heptyl radicals is abbreviated because these homologs have the same geometry beyond the β-carbon. Frequency calculations were performed to determine the nature of stationary points, and to obtain ZPE (zero point energy) for accurate energy barriers and analytical force constants. ZPE with 0.9 correction was used for UHF whereas the 1.0 ZPE correction was applied to the

TABLE I.
Calculated Bond Lengths of Octane and Resulting Radicals.

	Methyl radical			
Bond lengths (Å)	Full-opt UB-I	Full-opt UHF-I	UMP2/6-311G*	Exp.[b]
C1H2	1.082	1.073	1.079	1.079
C1H3	1.082	1.073		
C1H4	1.082	1.073		

TABLE I.
(Continued)

Ethyl radical

Bond lengths (Å)	Full-opt UB-I	Full-opt UHF-I	UMP2 / 6-311G**[a]
C1H3	1.096	1.086	1.093
C1H4	1.096	1.086	
C1H5	1.105	1.091	1.099
C2H6	1.085	1.075	1.082
C2H7	1.085	1.075	
C1C2	1.490	1.498	1.492

Propyl radical

Bond lengths (Å)	Full-opt UB-I	Full-opt UHF-I	ROHF / 6-31G*[c]
C3H10	1.096	1.085	1.085
C3H9	1.097	1.085	1.085
C3H8	1.096	1.086	1.086
C2H6	1.100	1.087	1.087
C2H7	1.107	1.092	1.091
C1H4	1.086	1.076	1.076
C1H5	1.087	1.076	1.076
C1C2	1.492	1.500	1.501
C2C3	1.536	1.530	1.530

Butyl radical

Bond lengths (Å)	Full-opt UB-I	Full-opt UHF-I	ROHF / 6-31G*[c]
C3H10	1.098	1.088	1.087
C3H9	1.099	1.089	1.088
C2H8	1.100	1.088	1.088
C2H7	1.108	1.093	1.092
C1H6	1.087	1.076	1.075
C1H5	1.086	1.076	1.076
C1C2	1.492	1.500	1.501
C2C3	1.539	1.532	1.532

Pentyl radical

Bond lengths (Å)	Full-opt UB-I	Full-opt UHF-I
C3H11	1.099	1.088
C3H10	1.099	1.088
C2H9	1.010	1.088
C2H8	1.010	1.088
C1H7	1.086	1.076
C1H6	1.086	1.076
C1C2	1.492	1.501
C2C3	1.551	1.539

TABLE I.
(Continued)

Hexyl radical

Bond lengths (Å)	Full-opt UB-I	Full-opt UHF-I
C3H12	1.100	1.088
C3H11	1.099	1.088
C2H10	1.107	1.088
C2H9	1.100	1.088
C1H8	1.087	1.076
C1H7	1.086	1.076
C1C2	1.492	1.501
C2C3	1.539	1.539

Heptyl radical

Bond lengths (Å)	Full-opt UB-I	Full-opt UHF-I
C3H13	1.100	1.088
C3H12	1.099	1.088
C2H11	1.108	1.088
C2H10	1.100	1.088
C1H9	1.087	1.076
C1H8	1.086	1.076
C1C2	1.492	1.501
C2C3	1.538	1.538

n-Octane

Bond lengths (Å)	Full-opt Becke 3LYP	Full-opt HF-I	Exp.[d]
C2H3	1.097	1.086	1.150
C2H4	1.097	1.086	1.070
C2H5	1.096	1.086	0.930
C1H7	1.099	1.088	1.030
C1H8	1.099	1.088	1.080
C6H9	1.100	1.089	1.020
C6H10	1.100	1.089	1.030
C11H13	1.100	1.089	0.970
C11H14	1.100	1.089	1.120
C1C2	1.532	1.529	1.534
C1C6	1.534	1.530	1.522
C6C11	1.534	1.530	1.529
C11C12	1.534	1.530	1.516

[a] *Ab initio* UMP2 / 6-311G** results.[3]
[b] Values from ref. 32.
[c] *Ab initio* ROHF / 6-31G* results.[4]
[d] X-ray diffraction results of the octane crystal structure.[33]

TABLE II.
Calculated Bond Angles of Octane and Resulting Radicals.

Methyl radical

Angles (degrees)	Full-opt UB-I	Full-opt UHF-I	UMP2 / 6-311G*	Exp.[c]
H2C1H3	120.0	120.0	120.0	120.0
H2C1H4	120.0	120.0	120.0	
H3C1H4	120.0	120.0	120.0	
γ	0.0	0.0	0.0	

Ethyl radical

Angles (degrees)	Full-opt UB-I	Full-opt UHF-I	UMP2 / 6-311G**[a]
H7C2H6	117.4	117.2	117.6
C1C2H7	120.9	120.4	
C1C2H6	120.9	120.4	120.5
C2C1H5	112.1	111.7	111.4
C2C1H3	111.8	111.3	111.7
C2C1H4	111.8	111.3	
H3C1H4	108.0	107.9	108.2
H3C1H5	106.4	107.1	107.0
H4C1H5	106.4	107.1	
Dihedral angles (degrees)			
H6C2C1H5	−85.0	−81.9	
H7C2C1H5	85.0	81.9	
γ	8.7	14.0	11.9

Propyl radical

Angles (degrees)	Full-opt UB-I	Full-opt UHF-I	ROHF / 6-31G*[b]
H4C1H5	117.5	117.1	116.3
C2C1H4	121.1	120.3	119.3
C2C1H5	120.6	120.3	119.6
C1C2C3	113.6	113.1	112.9
C1C2H6	109.8	109.5	109.8
C1C2H7	110.0	109.5	109.6
Dihedral angles (degrees)			
C1C2C3H8	178.2	−180.0	−179.5
C1C2C3H9	58.3	59.9	60.2
C1C2C3H10	−61.3	−59.9	−59.6
C3C2C1H4	158.8	81.3	164.4
C3C2C1H5	−31.8	−81.2	−40.9
H4C1C2H6	35.2	−40.5	42.0
H4C1C2H7	−79.6	−157.0	−73.6
H5C1C2H7	90.0	40.5	
H5C1C2H6	−155.1	157.0	
γ	8.8	15.1	

TABLE II.
(Continued)

Butyl radical

Angles (degrees)	Full-opt UB-I	Full-opt UHF-I	ROHF / 6-31G*[b]
H5C1H6	117.5	117.2	116.3
C2C1H5	121.2	120.5	119.4
C2C1H6	120.6	120.2	119.6
C3C2C1	113.8	113.2	113.2
C1C2H7	110.1	109.9	109.9
C1C2H8	109.9	109.4	109.4
H7C2H8	104.8	105.7	105.7
H9C3H10	106.2	106.4	
Dihedral angles (degrees)			
C1C2C3C4	178.3	179.3	−179.9
C3C2C1H5	156.0	159.9	163.7
C3C2C1H6	−34.0	−37.0	−41.3
C1C2C3H9	56.2	57.3	57.6
C1C2C3H10	−59.2	−58.5	−58.2
H7C2C1H5	−82.3	−78.2	−74.3
H7C2C1H6	87.7	85.0	80.6
H8C2C1H5	32.7	37.4	41.3
H8C2C1H6	−157.3	−159.4	−163.7
γ	8.6	14.5	

Pentyl radical

Angles (degrees)	Full-opt UB-I	Full-opt UHF-I
H6C1H7	117.3	117.1
C2C1H6	120.9	120.4
C2C1H7	120.9	120.4
C3C2C1	113.7	113.4
C1C2H8	110.0	109.5
C1C2H9	110.0	109.5
H8C2H9	106.5	106.5
H10C3H11	106.2	106.3
Dihedral angles (degrees)		
C1C2C3C4	−180.0	−180.0
C2C3C4C5	180.0	180.0
C3C2C1H6	84.1	81.5
C3C2C1H7	−84.2	−81.6
C1C2C3H10	57.8	57.9
C1C2C3H11	−57.8	−57.9
H8C2C1H6	−154.4	−156.7
H8C2C1H7	37.2	40.2
H9C2C1H6	−37.4	−40.2
H9C2C1H7	154.3	156.7
γ	10.0	14.6

TABLE II.
(Continued)

Hexyl radical		
	Full-opt	
Angles (degrees)	UB-I	UHF-I
H7C1H8	117.5	117.0
C2C1H7	121.2	120.4
C2C1H8	120.6	120.4
C3C2C1	113.7	113.4
C1C2H9	109.9	109.5
C1C2H10	110.1	109.5
H9C2H10	104.8	106.5
H11C3H12	106.1	106.3
Dihedral angles (degrees)		
C1C2C3C4	−178.8	−180.0
C3C4C5C6	179.8	−180.0
C3C2C1H7	−156.1	−81.5
C3C2C1H8	34.0	81.5
C1C2C3H11	58.8	57.9
Ca1C2C3H12	−56.6	−57.9
H9C2C1H7	−32.8	40.3
H9C2C1H8	157.2	−156.7
H10C2C1H7	82.2	156.7
H10C2C1H8	−87.7	−40.3
γ	8.6	14.6

Heptyl radical		
	Full-opt	
Angles (degrees)	UB-I	UHF-I
H8C1H9	117.5	117.1
C2C1H8	121.2	120.4
C2C1H9	120.6	120.4
C3C2C1	113.8	113.4
C1C2H10	109.9	109.5
C1C2H11	110.1	109.5
H10C2H11	104.8	106.4
H12C3H13	106.1	106.3
Dihedral angles (degrees)		
C1C2C3C4	−178.6	−180.0
C4C5C6C7	180.0	180.0
C3C2C1H8	−156.8	−81.5
C3C2C1H9	33.2	81.5
C1C2C3H12	58.9	57.9
C1C2C3H13	−56.5	−57.9
H10C2C1H8	−33.5	40.3
H10C2C1H9	156.5	−156.7
H11C2C1H8	81.5	156.7
H11C2C1H9	−88.5	−40.3
γ	8.6	14.6

TABLE II.
(Continued)

n-Octane			
	Full-opt		
Angles (degrees)	Becke 3LYP-I	HF-I	Exp.[d]
H3C2H4	107.5	107.6	104.0
H3C2H5	107.7	107.7	118.0
H4C2H5	107.7	107.7	110.0
H7C1H8	106.0	106.2	113.0
H9C6H10	105.9	106.2	108.0
H13C11H14	105.9	106.2	115.0
H3C2C1	111.2	111.1	
H4C2C1	111.2	111.1	
H5C2C1	111.5	111.3	
H7C1C2	109.5	109.3	
H8C1C2	109.5	109.3	
H9C6C1	109.2	109.2	
H10C6C1	109.2	109.2	
H13C11C6	109.2	109.3	
H14C11C6	109.2	109.3	
C2C1C6	113.3	113.0	114.4
C1C6C11	113.6	113.3	113.3
C6C11C12	113.6	113.3	112.2
Dihedral angles (degrees)			
H5C2C1C6	180.0	180.0	
C6C11C12C16	180.0	180.0	
C16C18C23H24	−180.0	180.0	
H3C2C1C6	59.8	59.9	
H4C2C1C6	−59.8	−59.9	
H7C1C2H5	57.9	58.0	
H8C1C2H5	−57.9	−58.0	
H9C6C1C2	57.7	−57.9	
H10C6C1C2	−57.7	−57.9	
H13C11C6C1	57.7	57.9	
H14C11C6C1	−57.7	−57.9	

[a] *Ab initio* UMP26-311G** results.[3]
[b] *Ab initio* ROHF 6-31G* results.[4]
[c] Values from ref. 32.
[d] X-ray diffraction results of the octane crystal structure.[33]

DFT energetics. At the optimized geometries, the force constants, harmonic frequencies, and infrared intensities were determined by analytical differentiation of the SCF wave functions and by numerically differentiating the analytical first derivatives of the UMP energies (where UMP is UMP3, UMP2/6-31G*//UHF/6-31G*). Vibrational frequencies and energy values are shown in Tables III and IV. Restricted Becke 3LYP/6-31G* with ZPE corrections (hereafter referred to as RB) was used on the closed-shell octane. For the less meaningful

TABLE IIIA.
Approach I: Selected Unscaled Vibrational Frequencies (cm^{-1}).

	UHF-I		UB-I		UMP2 / 6-311G**[a]		
Vibrational mode	Symmetry	Frequency	Symmetry	Frequency	Symmetry	Frequency	Observed
Methyl radical (C_{2v})							
CH3 asymm. str.	E′	3461	A1	3321	E′	3372	3162[a]
			B2	3322			
CH3 symm. str.	A1′	3284	B2	3146	A1′	3179	
CH3 out-of-plane bend	A2″	308	B1	449	A2′	424	617[a]
Ethyl radical (C_s)							
α-CH2 asymm. str.	A	3412	A″	3271	A″	3325	3112[a,b]
α-CH2 symm. str.	A	3314	A′	3174	A′	3214	3033[a,b]
α-CH3 asymm. str.	A	3264	A″	3107	A″	3175	2987[a,b]
	A	3229	A′	3062	A′	3129	2920[a,b]
CH3 symm. str.	A	3161	A′	2965	A′	3045	2842[a,b]
α-C—C str.	A	1113	A′	1074	A′	1094	1138[a,b]
α-CH2 pyramidal bend	A	462	A′	450	A′	458	540[a,b]

[a] Values from ref. 3a.
[b] Values from ref. 3d.

TABLE IIIB.
Approach I: Selected Unscaled Vibrational Frequencies (cm^{-1}).

Heptyl radical (C_1)[a,b]

	UHF-I		UB-I	
Vibrational mode	Symmetry	Frequency	Symmetry	Frequency
α-CH2 asymm. str.	A″	3404	A	3257
α-CH2 symm. str.	A′	3307	A	3160
CH3 asymm. str.	A″	3259	A	3110
CH3 symm. str.	A′	3198	A	3041
α-C—C str.	A′	1137	A	1093
α-CH2 pyramidal bend	A′	559	A	410
			A	458
			A	491

n-Octane (C_{2h})

	RHF-I		Becke 3LYP-I		
Vibrational mode	Symmetry	Frequency	Symmetry	Frequency	Observed[c]
CH3 asymm. str.	A″	3260	Bu	3108	2964
CH2 asymm. str.	A″	3238	Au	3073	2930
CH3 symm. str.	A′	3260	Bu	3039	2880
CH2 symm. str.	A′	3193	Bu	3028	2865

[a] No experimental vibrational frequency data.
[b] C_1 point group produced A-symmetry vibrational bands.
[c] Values from refs. 34 and 35.

TABLE IVA.
Carbon—Carbon Bond Dissociation Energies (BDE in kcal / mol) of Approaches I and II at 298.15 K.

Reaction	UB-I[a]	UMP2-I[b]	UMP3-I[c]	UB-II[a]	UMP2-II[b]	UMP3-II[c]	Exp.[d]
C8 → C1 + C7	86.5	92.1	88.1	105.0	108.4	104.9	87.77
C8 → C2 + C6	83.5	92.5	87.9	102.3	110.4	106.1	85.84
C8 → C3 + C5	83.7	93.3	88.6	102.8	111.2	106.8	85.56
C8 → C4 + C4	83.9	93.1	88.3	102.7	111.2	106.8	85.34

[a]UBECKE 3LYP / 6-31G* results. Energies include ZPVE.
[b]UMP2 / 6-31G* / / UHF / 6-31G* results. Energies include ZPVE * (0.89).
[c]UMP3 / 6-31G* / / UHF / 6-31G* results. Energies include ZPVE * (0.89).
[d]Experimental energies derived from the modified additivity scheme at 298.15 K.

TABLE IVB.
Comparisons of Calculated and Experimental Heats of Formations of Radicals in the Bond Rupture of Octane.

	UB[a]	UMP2[b]	UMP3[c]	Additivity[d]	Exp.[d]	ΔH_f^0 (UB)[e]	ΔH_f^0 (UMP3)	ΔH_f^0 (additivity)
C1 + C7	86.5	92.1	88.1	87.8	87.8	C1: 33.39	34.99	34.66
C2 + C6	83.5	92.5	87.9	85.9	85.8	C2: 27.69	31.09	27.8
C3 + C5	83.7	93.3	88.6	83.8	85.6	C3: 22.61	24.21	22.7
C4 + C4	83.9	93.1	88.3	86.1	85.3	C4: 15.9	20.6	18.1
						C5: 11.1	26	11.19
						C6: 5.8	10.2	5.9
						C7: 0.9	2.5	3.21

[a]Energies in kcal / mol; Ubecke 3LYP / 6-31G*.
[b]UMP2 / 6-31G* / / UHF / 6-31G*.
[c]UMP3 / 6-31G* / / UHF / 6-31G*.
[d]298 K.
[e](i) Isodesmic: C1 + C7 = C2 + C6 = C3 + C5 = C4 + C4; (ii) C8H18 = C2 + C6; (iii) De C8H18 = $\Sigma\Delta H_f^0$[(C2H5 + C6H13) − C8H18].

snapshot approach, the results on the C_{2h}-elongated octane are used to mimic the low tetrahedral early transition state of radical formation. Work on the radical states was carried out by full optimization at UB3LYP/6-31G* (hereafter referred to as UB-I) on the open-shell methyl (D_{3h}), ethyl (C_s), propyl, butyl, pentyl, hexyl, and heptyl (C_1) primary radicals. For the open-shell systems, the $\langle S^2 \rangle$ values, derived from the Kohn–Sham orbitals, never exceeded 0.754. All the energies and entropies were tabulated at the RB, RHF, UB, and UMP levels. Temperature and pressure variations of the UB-I entropies (Table V) were investigated at standard conditions (298.15 K and 1 atm) and 800 K and 130 atm pressure; the resulting free energies are tabulated in Table VI. Enthalpy temperature corrections for octane and the radicals were derived using calculated vibrational frequencies and standard statistical thermodynamics formulas.

Results and Discussion

The fully optimized geometries and vibrational frequencies using UHF, UMP, and UB, for C1 to C7 radicals are discussed here. The snapshot approach geometries in all methods applied are not representative of the final fully relaxed geometries, but their relative energy trends may prove useful with C30 hydrocarbons. In approach II, the snapshot approach, the molecular geometries of the radical products are ''frozen'' in the configuration of the optimized octane precursor. The C—C bond in octane is stretched to infinity, while keeping all

TABLE V.
UB-I Energies, Entropies, and $\langle S^2 \rangle$ for Octane and Resulting Radicals.

Molecule	HF energy (a.u.)	ZPE (a.u.)	S (e.u)	$\langle S^2 \rangle$
Methyl radical	−39.8383	0.0298	48.9	0.7538
Ethyl radical	−79.1579	0.0596	61.5	0.7540
Propyl radical	−118.4714	0.0887	68.5	0.7539
Butyl radical	−157.7853	0.1174	76.3	0.7539
Pentyl radical	−197.0988	0.1464	81.1	0.7540
Hexyl radical	−236.4127	0.1747	91.3	0.7540
Heptyl radical	−275.7264	0.2034	98.7	0.7539
Octane	−315.7129	0.2473	101.9	0.0000

other bond lengths and bond angles fixed. Here, fragment relaxation is not allowed to occur, whereas, in approach I, full optimization is performed. Ruchardt et al. have studied the pyrolysis free energies of activation and found them to resemble calculated molecular strain energies.[22] This

TABLE VI.
$\Delta G^0_{298\,K}$ and ΔG at 800 K and 130 atm Derived from UB-I Calculations in kcal / mol.

Dissociation reaction	$\Delta G^{1\,atm}_{298\,K}$	$\Delta G^{130\,atm}_{800\,K}$
C8 → C1 + C7	72.8	61.0
C8 → C2 + C6	68.3	54.6
C8 → C3 + C5	69.1	59.7
C8 → C4 + C4	68.7	55.1

is in accord with the Hammond postulate, where the transition state is expected to lie near the product of the exothermic reaction. The basis of the snapshot approach is the proximity of the difference in strain energies between the saturated hydrocarbons and the resulting dissociation radicals. Because the snapshot approach is a general representation of bond elongation in octane, examples are displayed in Figures 1–3 along with the fully optimized UB results.

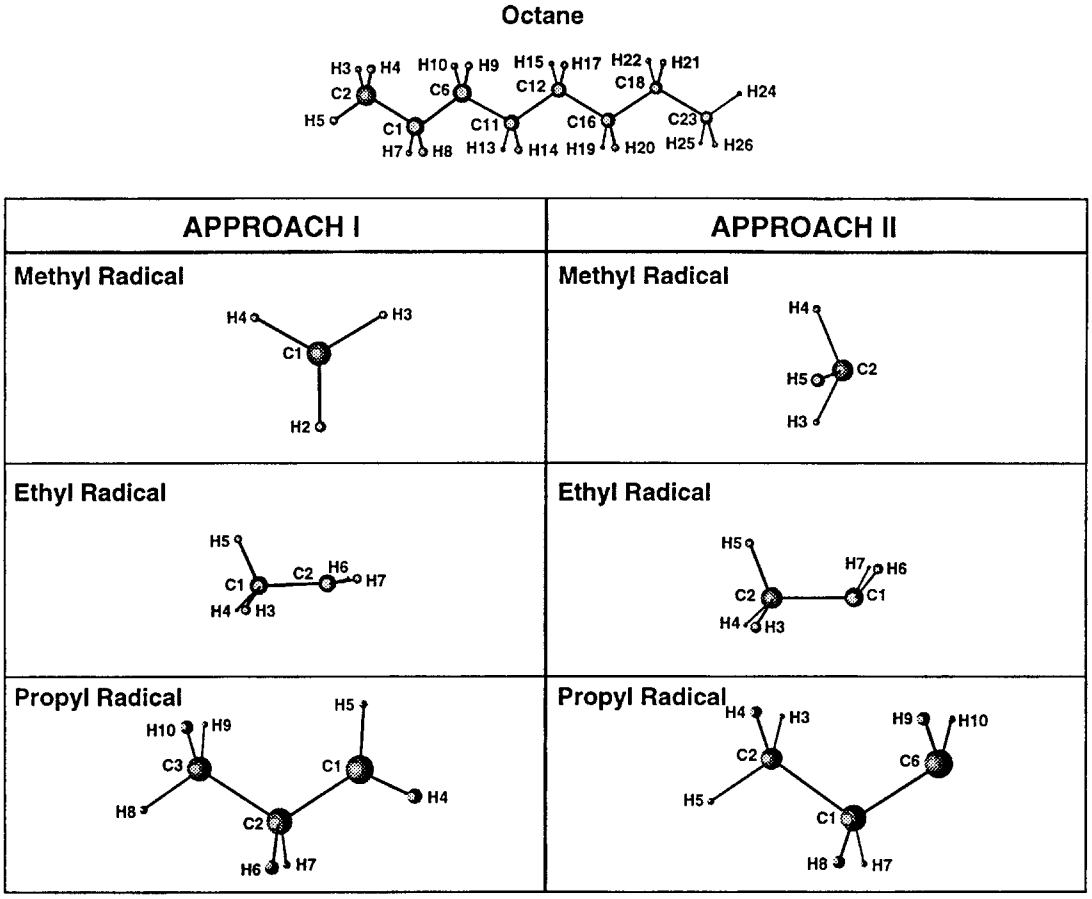

FIGURE 1. Fully optimized approach (I) and the snapshot approach (II): molecular geometries of octane and the radicals fragments.

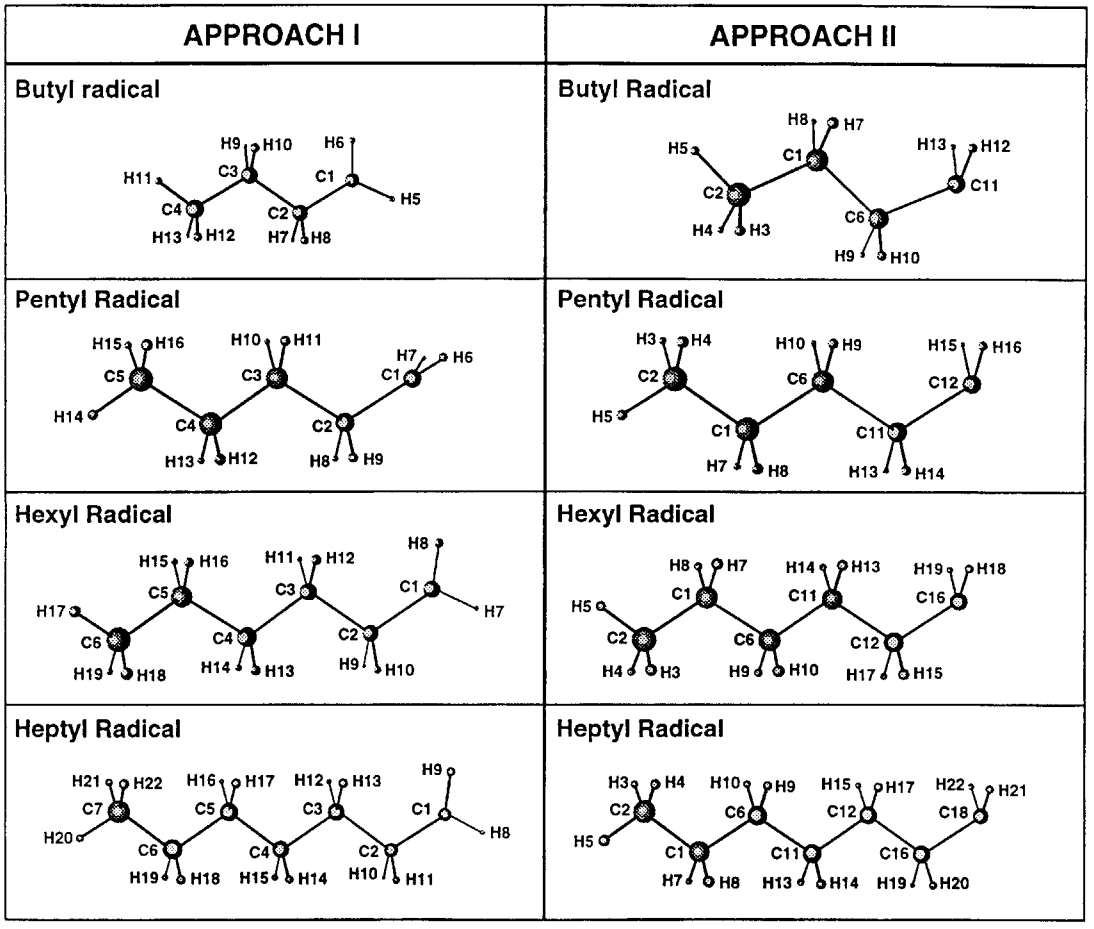

FIGURE 2. Approach I and II molecular geometries of the radicals fragments.

The scission of a bond in the main chain to produce two radical centers is clarified by the DFT vibrational details, which are displayed in Table III. For the energy results, comparisons of both approaches I and II are included; Table IVA includes ZPE-corrected energies for the UMP and UB methods. Table IVB summarizes UB, UMP, additivity estimates, and experimental results of the octane bond rupture. Table V includes fully optimized UB energies, ZPE, entropies, and spins. Table VI focuses on the corresponding UB free energies.

Geometry and Vibrational Frequencies

The results for the geometry optimization of methyl, ethyl, propyl, butyl, pentyl, hexyl, and heptyl radicals are summarized in Tables I and II and illustrated in Figures 1 and 2.

UHF results (Table I) indicate the methyl radical is planar with a D_{3h} symmetry with 120° angles. This agrees with optical and electron spectroscopy which has established methyl radical planarity.[23] Early large-scale configuration interaction calculations also confirmed this with a single minimum out-of-plane bending coordinate.[24] In contrast to UHF, UB shows a C_{2v} symmetry due to an elongated C—H bond and 120° angles. UHF is in satisfactory agreement with Pacansky's MP2/6-311G**-optimized results (1.072 Å).[3a,e]

The semistaggered conformation of the ethyl radical reflects the van der Waals repulsions between the hydrogens of the methylene groups and the methyl (planar) fragment. Matrix isolation studies have shown that the ethyl radical may be taken to be nearly planar, with the trigonal carbon having considerable sp^2 character.[3e] The out-of-plane bending frequency of 449 cm^{-1} (UB) (Table III) may be due to either anharmonicity or the Jahn–Teller effect.[3a,4b] The deviations from the 617 cm^{-1} experimental value have improved by over 30 cm^{-1} in the UB approach compared with UHF/6-311G** results.

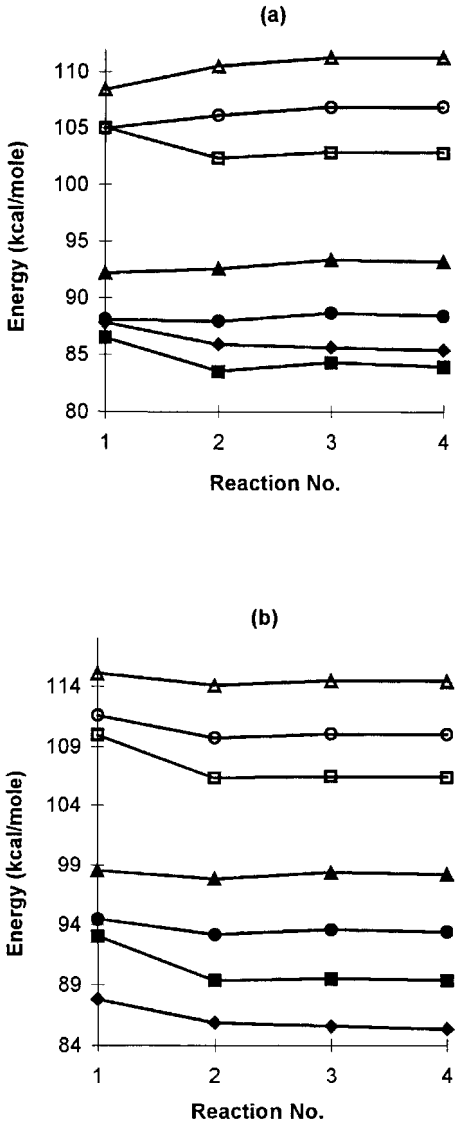

FIGURE 3. (a) Bond dissociation energies at 298 K. (b) Bond dissociation energies with no enthalpy or zero-point energy corrections. Reaction number 1 (RN1) represents carbon–carbon bond cleavage of octane to form the methyl and heptyl radicals. RN2 corresponds to the ethyl and hexyl formations. RN3 corresponds to the propyl and pentyl formations. RN4 corresponds to the formation of two butyl radicals. (△) Snapshot UMP2 / 6-31G* // UHF / 6-31G* results; (○) snapshot UMP3 / 6-31G* // UHF / 6-31G* results; (□) snapshot Ubecke 3LYP / 6-31G* results; (▲) full-opt UMP2 / 6-31G* // UHF / 6-31G* results; (●) full-opt UMP3 / 6-31G* // UHF / 6-31G* results; (■) full-opt Ubecke 3LYP / 6-31G* results; (♦) experimental as well as values derived from the modified additivity method.

Both methods produced ethyl radical structures similar to ethane, with the β-CH bond trans to the unpaired electron in the fully optimized approach. The out-of-plane pyramidal angle is 8.8° in UB. This closely matches the 8.3° dihedral in recent MM3 studies,[4b] but appears smaller than the 9.7° from MM2 results and the *ab initio* UHF/6-311G** value of 11.9°.[4e,d] The ethyl radical frequency for inversion in the UB approach (450 cm^{-1}) is low compared with the experimental value of 540 cm^{-1}.[25] The 551 cm^{-1} MM3 value[4b] is more accurate than the 435 cm^{-1} finding from SUMP2/6-311G**[3d] results, and provides strong support for the force field approach in deriving inversion energies.

The UB structural features agree with previous *ab initio* results for the higher primary alkyl radicals. The C—C distances are shorter than the MM3 values by less than 0.05 Å, whereas C—H bonds are 0.03 Å shorter than the more extended basis and ROHF *ab initio* results and MM3 calculations.[4b] Most of the UB bond angle results agree with MM3 and *ab initio* results to within 1°,[3,4] with larger deviations occurring for the torsional out-of-plane angle. The only significant deviation in the C—C—C angle in the propyl radical, extending to more than 2°, occurs when comparing UB with MM3 calculations.[4b]

Butyl radical UB geometric features are also summarized in Tables I and II. The average C—H bond length in UB-I is 1.086 Å, which corresponds more closely to the MM3 average C—H bond length than previous *ab initio* studies.[4b] The α-C—H bond retains the tight 1.076 Å length compared with the β-C—H of 1.09 Å, whereas angular features deviate by less than 1° from the MM3 results. The dihedral angle for the lowest conformer is 8.6°. This shows a consistent trend within the smaller radicals, and illustrates the van der Waals repulsions of the methyl groups added to the radical.

There is little quantitative information in the literature on the *n*-pentyl free radical. The isomerization via 1,4-hydrogen-atom transfer is better documented in C6 and C7 alkyl radicals than for the pentyl group.[26] The C—H bond α to the radical center in the pentyl radical is shorter by 0.04 Å than the other higher radicals and exceeds the propyl bond by 0.08 Å. In short, as seen in Table I, it is more like the ethyl α-C—H bond. The pentyl radical has an irregular dihedral angle of 10.0° which demonstrates the increased repulsion of the added methyl group on the radical end. It is possible that, if all low-lying conformers are in-

cluded, this deviation would not occur, as is the case in the hexyl and heptyl case.

The infrared spectra of the radicals reveal that the vibrational modes are separated into two types: one with modes that typify the radical center, and the other characteristic of vibrations of the nonradical portion, similar to closed-shell primary alkanes. The calculated frequencies of the β-C—H bonds in alkyl radicals are considerably weaker than other CH bonds, and the observed red shift in the vibrational spectrum is compared for ethyl to pentyl radicals. For example, the ethyl radical has absorption at 2840 cm^{-1}, which is characteristic for a CH bond in a β position to the radical center.

Pacansky's work on IR of the butyl radical is typified by the —CH2 stretches at 3105 cm^{-1}, β-CH2 stretches at 2835 cm^{-1}, and the radical umbrella mode at 520 cm^{-1}.[27] Our UB results agree closely with an umbrella mode of 450 cm^{-1}. Both butyl and pentyl radicals have absorptions at 3105 and 3025 cm^{-1} which are assigned to the asymmetric and symmetric stretching modes of the α-C—H bond.

DFT vibrational results in the 1350–1370 cm^{-1} region, for C2–C7 radicals, are in excellent agreement with the terminal methyl group rocking motion in primary alkanes, which occurs at 1378 cm^{-1}, and is virtually independent of chain length. This vibrational feature will shed light on predictions related to alkanes that are used as solvents.[28]

Energies of Radicals and Bond Rupture

In assessing the performance of hybrid DFT methods in predicting the gas phase pyrolysis of octane, systematic errors are detailed first. UB3LYP/6-31G* overestimates the C—H bond energies by 0.8 kcal/mol when compared with previous molecular mechanics, *ab initio* results, and experimental results.[4b,5,7] Similarly, the C—C bond energies are underestimated by 2–3 kcal/mol as seen by Hay in the study of heats of atomizations.[29] A systematic error related to hybrid functional zero-point vibrational energy correction (ZPE) is the 4–5% higher UB data, when compared with experimental values. The UHF frequencies are typically overestimated by 10% for the zero-point energies. As mentioned previously, neglecting the conformational mixings possible at RT, especially in the case of butyl–heptyl radicals, also incurs an error of close to 0.5 kcal/mol. The average net uncertainty in energies from all of the above factors lies below 3 kcal/mol. This matches an uncertainty of 2–3 kcal/mol in the modified additive bond energies. The energetic trends are illustrated in Figure 3 for all approaches studied.

At 298 K, the bond dissociation energies of the UB are 1–2 kcal below the simple additivity scheme values (Fig. 3a and Table IVA). Density functional results match the trend closely, with two exceptions: the butyl radical (C4—C4) is lower than the predicted values, whereas the pentyl radical (C5—C3) appears slightly higher. When UHF energy results are improved with MP3 correlation, they still show a poor mimicry of the energetic pattern typified by the smoothing out at the butyl, pentyl, and hexyl stages. The only reasonable UMP3 result is the C1—C7 rupture, which is comparable with the available data. Thus, the UB results are both computationally more efficient and more accurate than the UMP3 work. UMP2 results show the same trend as the UMP3-correlated values but deviate energetically by over 6 kcal/mol for all bond ruptures.

The attempted mimicry of the bond rupture *trend* is barely achieved with the UB snapshot approach, because energy deviations exceed 20 kcal/mol. Again, this approach is not used to elucidate the energies but simply to assess its ability in finding the weakest bond in C30 and larger hydrocarbons. It appears that, with today's high-accuracy DFT calculations, the snapshot approach is not sensitive enough to consider further. This calculation indicates that the DFT hybrid approach is better in matching experimental and predicted radical energies than the correlated UHF approach. With a more extensive basis set, it is possible that these results will converge more closely.

Table IVB indicates that UB bond rupture deviates from experiment by no more than 2 kcal/mol. With the aid of the isodesmic octane rupture into radicals, C1 + C7, C2 + C6, C3 + C5, C4 + C4, and the equation, D (C8H18) = ΔH_f^0 {(C2H5 + C6H13) − (C8H18)}, for example, calculated values for the heats of formation of radicals are obtained. This is done with the use of two known heats of formation—in the above equation, C8H18 and C2H5, to obtain the hexyl radical computed heat of formation. As Table IVB indicates, UB results match the Benson additivity values to within 2 kcal/mol. The only deviations (2.2 kcal/mol) are the UB ΔH_f^0 of the butyl and heptyl radicals. This may be due to the neglect of confor-

mational and population effects in these two radicals. The UMP3 method generally deviates by up to 3 kcal/mol. The two series deviations include the heptyl and hexyl radicals, for the same reasons stated previously. Predicting heats of formations of alkyl primary radicals, appears to be one useful result of this study.

Free Energies and Entropies

For each bond rupture, the standard free energy at 298.15 K and 800 K is determined. The calculated free energies have not been optimized (the energies of the radicals have) and thus this extension of the data may be somewhat erroneous.[30] It could, however, present some insight into the entropy of the bond rupture at the geothermally significant temperature and pressure conditions.

UB results at 298 K show that, in spite of a close energetic match with experimental predictions, the calculated free energies become more linear. Seetula et al. have shown that the heats of formations of alkyl radicals are more accurate using the third law method than second law approximations.[2] This is due to the second law being very sensitive to the accuracy of the activation energies involved. The third law approach is relatively insensitive to experimental activation energies but relies on the accuracy of calculated entropies. Thus, third law results are close to 0.5 kcal/mol, whereas second law results deviate by 2.5 kcal/mol. Table VI shows the second law results at 298 K and 1 atm, and compares the results at 800 K and 130 atm. UHF methods are more linear than UB results at 298 K. The oil reservoir conditions simulated in our final UB work indicate a closer correlation with experimental data, and entropic increases in all radicals other than methyl are evident. The C1−C7 differs by 2 kcal/mol, both computationally and experimentally, from all of the resulting radicals. This yields evidence that, under these higher temperature and pressure conditions, the first methyl bond rupture occurs with greater ease. Also present in reservoirs, as suggested by Basset et al. are transition metal hydride catalysts that convert alkanes to lower homologs and ultimately methane.[31] Indeed, at high temperature (T) and pressure (P) conditions with transition metal hydrides present, it is possible to see the extensive methane production occurring. Table VI also shows the entropic effects that result at high T and P and elucidates this phenomenon.

Conclusion

Hybrid DFT calculations with the 6-31G* basis match experimental data closely. Geometries and frequencies are improved with UB3LYP calculations relative to UHF results. The DFT UB results show methyl−heptyl bond rupture to be 5 kcal/mol higher, and the UB results are within the 2-kcal/mol uncertainty level of the empirical bond rupture scheme. In terms of energy trends, the UMP3, UMP2/6-31G*//UHF/6-31G* are least accurate, whereas UB3LYP/6-31G* yields the best results. If accuracy is the intent, then UB is far superior to other methods and this study can now be extended to secondary and tertiary alkanes and their bond ruptures. Work is in progress to use DFT methods to shed light on polymerization and petroleum production processes.

References

1. (a) D. A. Leathard and J. H. Purnell, *Annual Reviews in Physical Chemistry*, H. Eyring, C. J. Christensen, and H. S. Johnson, Eds., Palo Alto, CA, 1970, p. 197. (b) C. E. Hoyle and J. F. Kinstle, Eds., *Radiation Curing of Polymeric Materials*, American Chemical Society, Washington, DC, 1989; (c) W. Schnabel, *Polymer Degradation: Principles and Practical Applications*, MacMillan, New York, 1981.
2. (a) J. J. Russell, J. A. Seetula, R. S. Timonen, D. Gutman, and D. F. Nava, *J. Am. Chem. Soc.*, **110,** 3084 (1988); (b) D. F. McMillen and D. M. Golden, *Annu. Rev. Phys. Chem.*, **33,** 493 (1982).
3. (a) J. Pacansky, W. Koch, and M. D. Miller, *J. Am. Chem. Soc.*, **113,** 317 (1991); (b) H. R. Wendt and H. E. Hunziker, *J. Chem. Phys.*, **81,** 717 (1984); (c) G. Chettur and A. Snelson, *J. Phys. Chem.*, **91,** 5873 (1987); (d) J. Pacansky and M. Dupuis, *J. Am. Chem. Soc.*, **104,** 415 (1982); and references therein; (e) J. Pacansky and M. Dupuis, *J. Chem. Phys.*, **68,** 4276 (1978); (f) J. E. Leffler, *An Introduction to Free Radicals*, John Wiley & Sons, New York, 1993.
4. (a) M. Yoshimine, *J. Phys. Chem.*, **89,** 1880 (1985); (b) R. Liu and N. L. Allinger, *J. Comput. Chem.*, **15,** 283 (1994); (c) M. M. Iman and N. L. Allinger, *J. Mol. Struct.*, **126,** 345 (1985); (d) M. Guerra, *J. Am. Chem. Soc.*, **114,** 2077 (1992); (e) V. Kellö, M. Urban, J. Noga, and G. H. F. Diercksen, *J. Am. Chem. Soc.*, **106,** 5864 (1984); (f) B. T. Luke, G. H. Loew, and A. D. McLean, *J. Am. Chem. Soc.*, **109,** 1307 (1987).
5. (a) W. Tsang, *J. Am. Chem. Soc.*, **107,** 2872 (1985); (b) S. W. Benson, *Thermochemical Kinetics, 2nd Ed.*, John Wiley & Sons, New York, 1976; (c) N. Cohen and S. W. Benson, *Chem. Rev.*, **93,** 2419 (1993); (d) see, for example, G. Leroy and M. Sana, *Theochem*, **284,** 197 (1993), and references within.
6. (a) B. P. Tissot and D. H. Welte, *Petroleum Formation and Occurrence*, Springer, Berlin, 1978, p. 147; (b) F. Domine, *J. Am. Chem. Soc. Energy Fuels*, **3,** 89 (1989).

7. J. Pacansky, D. E. Horne, G. P. Gardini, and J. Bargon, *J. Phys. Chem.*, **81,** 2149 (1977).
8. (a) Y. Li and K. N. Houk, *J. Am. Chem. Soc.*, **115,** 7478 (1993); (b) E. Goldstein, B. Beno, and K. N. Houk, *J. Am. Chem. Soc.*, **118,** 6036 (1996).
9. (a) W. Kohn and L. J. Sham, *Phys. Rev.*, **140,** A1133 (1965); (b) P. Hohenberg and W. Kohn, *Phys. Rev.*, **136,** B864 (1964); (c) T. Ziegler, *Chem. Rev.*, **91,** 651 (1991); (d) J. Labanowski and J. Andzelm, Eds., *Density Functional Methods in Chemistry*, Springer, Berlin, 1991; (e) R. G. Parr and Y. Yang, *Density-Functional Theory of Atoms and Molecules*, Oxford University Press, New York, 1989.
10. B. G. Johnson, P. M. Gill, and J. A. Pople, *J. Chem. Phys.*, **98,** 5612 (1993).
11. See, for example: (a) K. N. Houk, Y. Li, J. Storer, L. Raimondi, and B. Beno, *J. Am. Chem. Soc. Faraday Trans.*, **90,** 1599 (1994); (b) D. Feller, E. D. Glendening, E. A. McCullough Jr., and R. J. Miller, *J. Chem. Phys.*, **99,** 2829 (1993); (c) I. Carmichael, *Coupled Cluster Meth. J. Chem. Phys.*, **91,** 1072 (1989), and references therein.
12. (a) B. S. Smith and L. Radon, *Chem. Phys. Lett.*, **231,** 345 (1994); (b) J. Andzelm and E. Wimmer, *J. Chem. Phys.*, **96,** 1280 (1992).
13. (a) C. W. Murry, N. C. Handy, and R. D. Amos, *J. Chem. Phys.*, **98,** 7145 (1993); (b) P. M. W. Gill, B. G. Johnson, J. A. Pople, and M. J. Frisch, *Int. J. Quant. Chem. Symp.*, **26,** 219 (1992).
14. (a) F. A. Houle and J. L. Beauchamps, *J. Am. Chem. Soc.*, **101,** 15 (1979); (b) R. J. Berry, D. R. F. Burgess Jr., M. R. Zachariah, C. F. Melius, and M. Schwartz, *J. Chem. Phys.*, **100,** 7405 (1996); (c) R. G. Snyder, M. Marocelli, and H. L. Straus, *J. Am. Chem. Soc.*, **105,** 133 (1983).
15. L. A. Curtiss, Ka., Raghavachari, G. W. Trucks, and J. A. Pople, *J. Chem. Phys.*, **94,** 7221 (1991).
16. J. D. Cox and G. Pilcher, *Thermochemistry of Organic and Organometallic Compounds*, Academic, London, 1970.
17. (a) J. A. Kerr, *Chem. Rev.* **66,** 465 (1966); (b) S. W. Benson, *J. Chem. Educ.*, **42,** 502 (1965).
18. J. L. Holmes, F. P. Lossing, and A. Maccoll, *J. Am. Chem. Soc.*, **110,** 7339 (1988).
19. M. J. Frisch, G. W. Trucks, H. B. Schlegel, P. M. W. Gill, B. G. Johnson, M. A. Robb, J. R. Cheeseman, T. A. Keith, G. A. Petersson, J. A. Montgomery, K. Raghavachari, M. A. Al-Latham, V. G. Zakrzewski, J. V. Ortiz, J. B. Foresman, J. Cioslowski, B. B. Stefanov, A. Nanayakara, M. Challacombe, C. Y. Peng, P. Y. Ayala, W. Chen, M. W. Wong, J. L. Andres, E. S. Replogle, R. Gomperts, R. L. Martin, D. J. Fox, J. S. Binkley, D. J. Defrees, J. Baker, J. J. P. Stewart, M. Head-Gordon, C. Gonzalez, and J. A. Pople, Gaussian, Inc., Pittsburgh, PA, 1995.
20. A. D. Becke, *J. Chem. Phys.*, **98,** 5648 (1993).
21. C. Lee, W. Yang, and R. G. Parr, *Phys. Rev. B*, **37,** 785 (1988).
22. C. Ruckardt and S. Weiner, *Tetrahed. Lett.*, 1311 (1979).
23. (a) G. Herzberg, *The Spectra and Structures of Simple Free Radicals*, Cornell University Press, Ithaca, NY, 1971; (b) G. B. Ellison, P. C. Enggelking, and W. C. Lineberger, *J. Am. Chem. Soc.*, **100,** 2256 (1978).
24. J. M. Marynick and D. A. Dixon, *Proc. Natl. Acad. Sci. USA*, **74,** 410 (1977).
25. E. Hirota, *J. Phys. Chem.*, **87,** 3375 (1983).
26. K. W. Watkins, *J. Am. Chem. Soc.*, **93,** 24 (1971).
27. J. Pacansky and A. Gutierrez, *J. Phys. Chem.*, **87,** 3074 (1983).
28. P. K. McCarthy and G. Blanchard, *J. Phys. Chem.*, **99,** 17748 (1995).
29. P. J. Hay, *J. Phys. Chem.*, **100,** 5 (1996).
30. K. Morokuma, W. T. Borden, and D. A. Hvorat, *J. Am. Chem. Soc.*, **110,** 4474 (1988).
31. M. Basset, *Science*, **271,** 966 (1996).
32. (a) G. Herzberg, *Mol. Spectra Molec. Struct.*, **2,** 344 (1945); (b) G. Herzberg, *Molec. Spectra Molec. Struct.*, **3,** 413, 646 (1966).
33. (a) H. Mathisen, N. Norman, and B. F. Pedersen, *Acta Chem. Scand.*, **21,** 9 (1967); (b) H. Mathisen, N. Norman, and B. F. Pedersen, *Acta Chem. Scand.*, **15,** 1747 (1961).
34. (a) *Spectrochem. Acta*, **19,** 117 (1963); (b) *Spectrochem. Acta*, **21,** 169 (1965).
35. W. M. Coleman III and B. M. Gordon, *Appl. Spectrosc.*, **43,** 1008 (1989).